Step Relaxation Method for Modal Test Implemented with Frequency-Domain Preprocessing

F. R. Vigneron* and Y. Soucy†
Communications Research Centre, Ottawa, Canada

The theory and practical aspects of an implementation of the step relaxation method of modal test that includes preprocessing of data in the frequency domain is presented. The method is demonstrated using a test of a continuous longeron space mast that has several low-frequency closely spaced modes.

Introduction

In the step relaxation method of modal test of structures, the input excitation is achieved by applying a single force to deform the structure statically and then releasing the force suddenly. Data acquired are the force history (for some implementations), and the ensuing structural response at a number of points measured before, during, and after release as the structure vibrates freely and damps to a motionless state. Data may also be obtained from successive reapplications of the force at the same and different locations and/or directions. The modal parameters are extracted from the input and output data using a parameter identification strategy. Several strategies for parameter identification with various time- and frequency-domain techniques are possible.[1-4]

This paper concentrates on the category of implementation where the structure's frequency-response function is first constructed in the frequency domain from the measured data, then inverted to the unit impulse response form in the time domain, and then the modal parameters are identified by fitting an analytic form of the unit impulse response function to the corresponding measurement-based function using the complex exponentials method.

This type of implementation of step relaxation is of interest because it is compatible with commercially available spectral analysis equipment, modal analysis software, and well-known spectral analysis data preprocessing techniques (prescreening of data at the Fourier transform level, frequency-domain averaging, etc.). Reference 4 reports on this implementation at an earlier stage of development and understanding.

The mathematical relationships, variables, and the frequency-response function are first established. Then several procedures for construction of the frequency-response function are discussed and demonstrated using test data from a lightweight flexible structure that is representative of the type for which step relaxation is well suited. The use of the polyreference implementation of the complex exponentials method of the Structural Dynamics Research Corporation's Modal-Plus software[5] is also illustrated with the representative data.

Mathematical Relationship Between Measurable Input and Output Variables and the Frequency-Response Function

To be compatible with frequency-domain parameter estimation hardware/software systems, one must first obtain an analytical expression that relates the measurable input and output variables to the frequency-response function.

A structure under step relaxation test is depicted schematically in Fig. 1. The standard mathematical model of the system is

$$M\ddot{x}+C\dot{x}+Kx=0 \tag{1a}$$

where x is an $n\times 1$ matrix of the deformation variables of the points specifying the geometry of the structure, and M, C, and K are corresponding mass, damping, and stiffness matrices, respectively. The structure is assumed to be preloaded with an applied set of forces and held in a static state, and then released at time $t=0$. Subsequent to release, Eq. (1a) and the initial conditions

$$x(0)=x_0 \text{ and } \dot{x}(0)=0 \tag{1b}$$

model the motion. The $n\times 1$ applied force matrix f_0 that initially deforms the structure is related to the initial condition by

$$f_0=Kx_0 \tag{2}$$

The measurable input and output variables are the scalar components of the restraining force and the accelerations a equal to $\ddot{x}$.

Although Eqs. (1) and (2) model the configuration completely, they are not in a form directly convenient for frequency-response methods of parameter estimation. Accordingly, they will be rearranged in the following. Transform from the variable $x(t)$ to $y(t)$, through

$$y(t)=x(t)-x_0 \tag{3}$$

Combining Eq. (3) with Eqs. (1) and (2) yields

$$M\ddot{y}+C\dot{y}+Ky=-f_0 \tag{4a}$$

$$y(0)=0 \text{ and } \dot{y}(0)=0 \tag{4b}$$

Define the step function $f(t)$, as

$$f(t)=-U(t)f_0 \tag{5}$$

where $U(t)$ is the standard unit step function[6,7] depicted in Fig. 2,

$$\begin{aligned} U(t)&=0, && t<0\\ &=\frac{1}{2}, && t=0\\ &=1, && t>0 \end{aligned} \tag{6}$$

Received Dec. 5, 1984; revision received May 24, 1985.

*Research Scientist. Member AIAA.
†Research Engineer. Member AIAA.

Then Eqs. (4) can be written as

$$M\ddot{y}+C\dot{y}+Ky=f(t) \tag{7a}$$

$$y(-\infty)=0 \text{ and } \dot{y}(-\infty)=0 \tag{7b}$$

The Fourier transform solution of Eqs. (7) is

$$\bar{y}(\omega)=\bar{H}(\omega)\bar{f}(\omega) \tag{8}$$

where $\bar{H}(\omega)$ is the frequency-response matrix (i.e., the transform of the unit impulse response matrix)

$$\bar{H}(\omega)=(-\omega^2M+i\omega C+K)^{-1} \tag{9}$$

From Eqs. (3) and (4b),

$$a(t)=\ddot{y}(t) \tag{10a}$$

$$\bar{a}(\omega)=-\omega^2\bar{y}(\omega) \tag{10b}$$

Combining Eqs. (8) and (10b), and writing the results in component form yields

$$\begin{bmatrix}\bar{a}_1(\omega)\\ \bar{a}_2(\omega)\\ \vdots\end{bmatrix}=-\omega^2\begin{bmatrix}\bar{H}_{11}(\omega) & \bar{H}_{12}(\omega) & \vdots\\ \bar{H}_{21}(\omega) & \bar{H}_{22}(\omega) & \vdots\\ \vdots & \vdots & \vdots\end{bmatrix}\begin{bmatrix}\bar{f}_1(\omega)\\ \bar{f}_2(\omega)\\ \vdots\end{bmatrix} \tag{11}$$

If the applied force has only one component, say f_k (i.e., $f_r=0$, $r\neq k$), then Eq. (11) can be recast into the form

$$\begin{bmatrix}\bar{H}_{1k}(\omega)\\ \bar{H}_{2k}(\omega)\\ \vdots\end{bmatrix}=-\frac{1}{\omega^2}\begin{bmatrix}\bar{a}_1(\omega)/\bar{f}_k(\omega)\\ \bar{a}_2(\omega)/\bar{f}_k(\omega)\\ \vdots\end{bmatrix} \tag{12}$$

The transform of $U(t)$ is[6]

$$\bar{U}(\omega)=\pi\delta(\omega)+\frac{1}{i\omega} \tag{13}$$

where $\delta(\omega)$ is the delta function.

Equation (12) demonstrates the mathematical relationship between the frequency-response function and the measurable input and output variables for a test configuration with a single applied force. One single applied force enables construction from measurements of one column of H. Additional columns can be constructed by successive tests with a force at additional single points.

Equation (11) can also be rearranged to allow construction of H from multiple-input force configurations of test.

The time history of the signal measured by a load cell located at the kth coordinate, $T(t)$, is shown in Fig. 3. It is related to $f_k(t)$ by

$$f_k(t)=T(t)-f_{0k} \tag{14}$$

The Fourier transforms of $f_k(t)$ and $T(t)$ are

$$\bar{f}_k(\omega)=-f_{0k}\left\{\pi\delta(\omega)+\frac{1}{i\omega}\right\} \tag{15}$$

$$\bar{T}(\omega)=-f_{0k}\left\{-\pi\delta(\omega)+\frac{1}{i\omega}\right\} \tag{16}$$

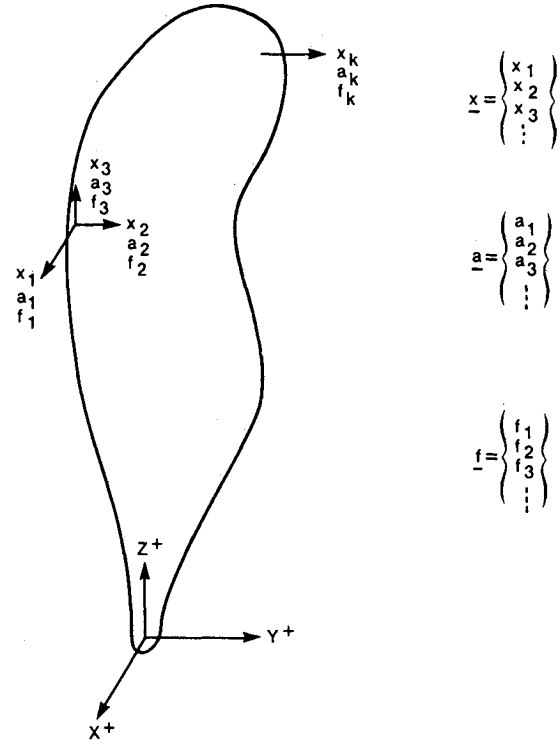

Fig. 1 Nomenclature for structure under step relaxation test.

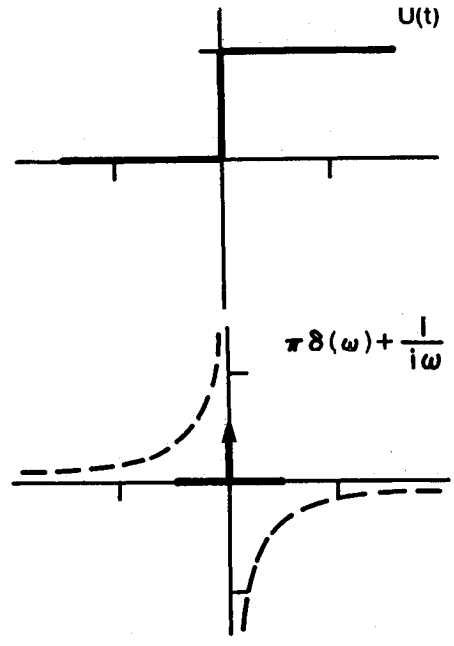

Fig. 2 Unit step function and its Fourier transform.

Experimental Data— Continuous Longeron Space Mast

Herein the data preprocessing associated with the preceding general theory, and the parameter estimation process, are illustrated with data from step relaxation tests of a continuous longeron space mast shown schematically in Fig. 4.

Nine instrument locations were defined on the structure, as depicted in the figure. In a particular test run, a single tangent force was applied and released with a solenoid-actuated release mechanism. The force was measured with a strain-gage-type load cell. Accelerations in the radial direc-

tions were measured first with a single force release (repeated three times and averaged, as described later), with nine accelerometers mounted to the structure. Then the accelerometers were turned to the tangential direction, and the releases were done to acquire tangent data. Axial deformations were known to be negligible from earlier tests and were not measured. In three sets of consecutive tests, the force was applied in the tangent direction at three of the nine instrument locations ($8y$, $-9y$, $11y$), with a view to later assembling the H matrix column by column as per Eq. (12).

The mass of the nine accelerometers was small but not negligible. However, with the above-described mounting strategy, the accelerometer mass was invariant at each location during the tests, the express purpose being to avoid lack of stationarity of the test configuration. Of the force release mechanism, only the load cell was attached to the structure. The mass of the load cell was about the same as the mass of one accelerometer. In previous tests, it was established that such a mass did not alter the frequency-response functions in the frequency range of interest. Thus moving the load cell from point to point did not induce nonstationarity.

The force application directions depicted in Fig. 4 were chosen to ensure that the data had good content of the two transverse bending and the torsion deformations. Thus the order of the deformation and H matrices was 18×1 and 18×3, respectively, in this particular example. Strip charts of typical analog force release and accelerometer output signals are shown in Fig. 5. The data acquisition was done with a GenRad 2503 system and Structural Dynamics Research Corporation's DATM software with appropriate specially written macros. The mast and test apparatus are described more fully in Ref. 8.

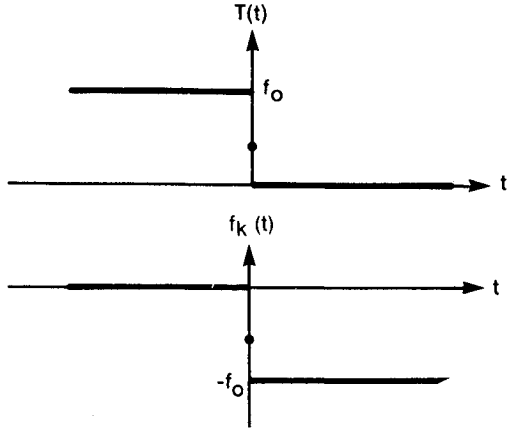

Fig. 3 *T(t)* **and** $f_k(t)$.

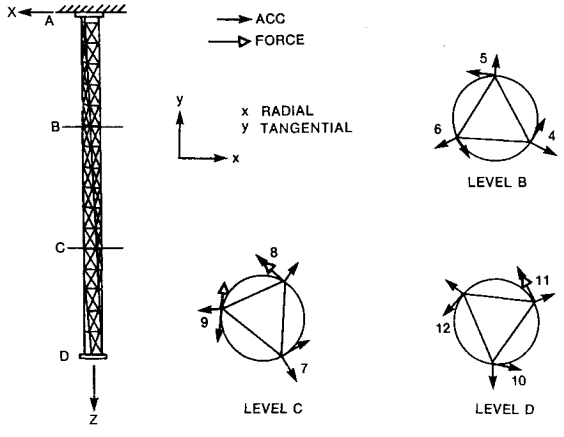

Fig. 4 Continuous longeron mast for step relaxation test.

Construction of the Measurement-Based Frequency-Response Function

The measurement-based frequency-response function, denoted $\bar{H}_{jk}(\omega_r)$, cannot be determined directly by dividing a fast Fourier transform (FFT) of the jth accelerometer signal by an FFT of a measurement-derived $f_k(t)$, as would appear to follow from Eq. (12), because of numerical problems associated with obtaining an FFT o $f_k(t)$. $f_k(t)$ involves the step function, and thus is not periodic nor of finite time duration. Consequently, a sampled data transform pair $\{f_k(t_r), \bar{f}_k(\omega_r)\}$ cannot be computed with a finite sampling window,[9] although the transform pair exists in the continuous domain as per Eqs. (14) and (15). References 2 and 4 describe two different signal processing techniques that overcome this difficulty.

The technique of Ref. 2 is depicted schematically for a single input force and one output accelerometer in Fig. 6. The voltage V_f that is proportional to $T(t)$ is passed through a high-pass analog filter. Because the filter passes only high frequencies, the dc component is eliminated and $V_{f1}(t)$ is equivalent to that which would be obtained by processing $f_k(t)$ [Eqs. (15) and (16)]. The resulting signal has a finite time duration and thus its Fourier transform can be computed numerically. The signal is then passed through an antialiasing filter that eliminates high-frequency noise effects (if any) and is sampled. Figure 7 shows the $V_{f2}(t_r)$ that corresponds to the $V_f(t)$ of Fig. 5. The accelerometer signals are passed through identical processing. From Fig. 6, one can represent the processing conceptually in the frequency domain as

$$\frac{\bar{V}_{a2}(\omega_r)}{\bar{V}_{f2}(\omega_r)} \sim \frac{\bar{G}_a(\omega)\bar{a}_j(\omega)}{\bar{G}_f(\omega)\bar{f}_k(\omega)} \tag{17}$$

If the analog filters are matched, $\bar{G}_a(\omega)/\bar{G}_f(\omega)$ reduces to unity, and $\bar{V}_{a2}(\omega_r)/\bar{V}_{f2}(\omega_r)$ is an appropriate approximation to $\bar{a}_j(\omega)/\bar{f}_k(\omega)$, [and, by Eq. (12), to an element of $\bar{H}(\omega)$]. Figure 8a shows an example of $\bar{a}_j(\omega_r)/\bar{f}_k(\omega_r)$ obtained with this method from a single trial with one applied input force. Figure 8b shows the same result obtained by averaging the results of three trials with the same input force configuration. This technique is effective, provided that the frequencies of interest are sufficiently high so as not to be eliminated by the G_a and G_f filters.

Reference 4 uses a digital linear transformation Z_s (rather than a high-pass analog filter), as shown in Fig. 9, where Z_s is defined by

$$V_f'(t_r) = V_f(t_{r-1}) - V_f(t_r) \tag{18}$$

Equation (18) is essentially a differentiation and eliminates the step from the signal. The $V_f'(t_r)$ derived from $T(t)$ as

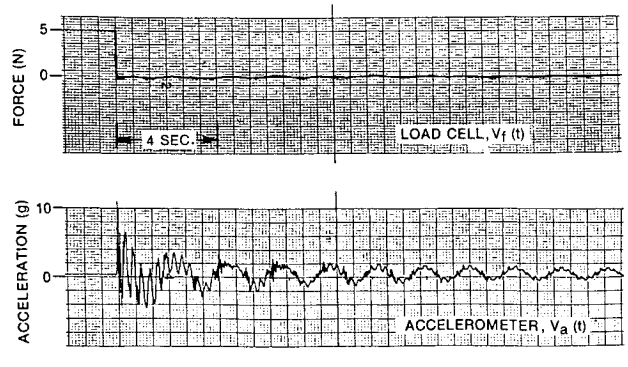

Fig. 5 Strip chart of analog signals during a typical release. Force proportional to $V_f(t)$. **Acceleration proportional to** $V_a(t)$.

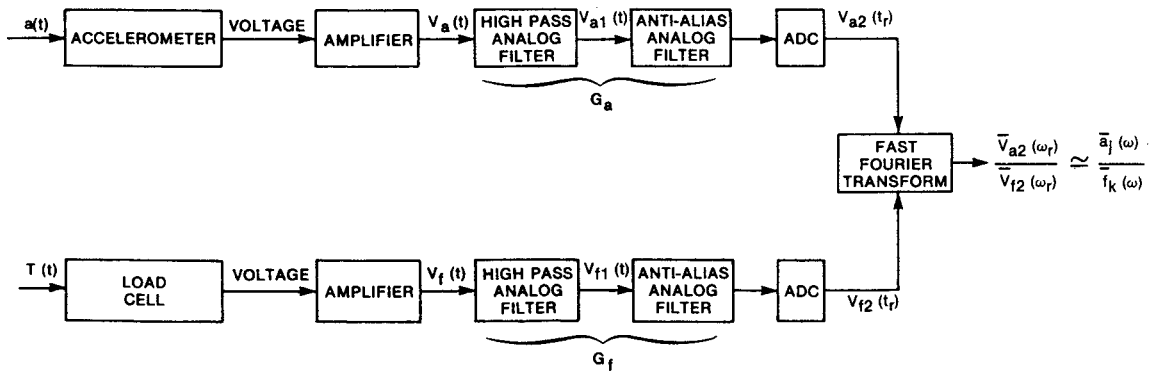

Fig. 6 Initial signal conditioning for step relaxation using high-pass analog filter.

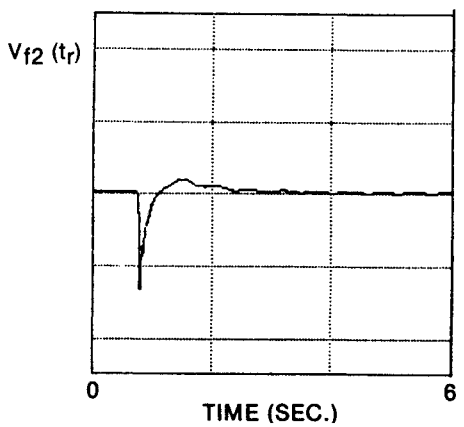

Fig. 7 Digitalized signal $V_{f2}(t_r)$.

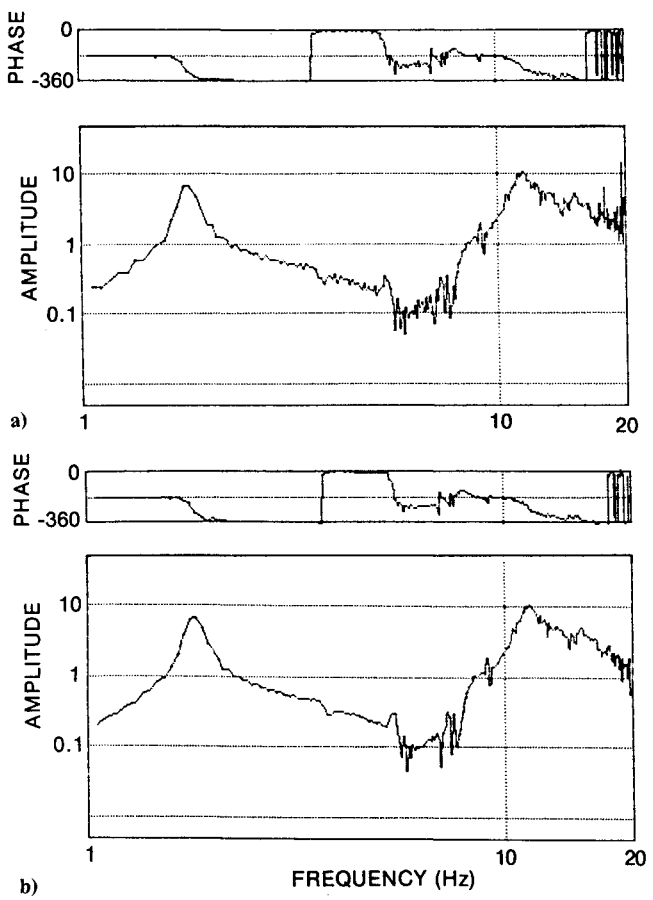

Fig. 8 $\bar{H}(\omega_r)$ obtained in step relaxation test: a) one trial, b) average of three trials.

per Fig. 9 is identical to that which would be derived from a linear transformation of $f_k(t)$ [$T(t)$ minus constant f_{0k}, by Eq. (14)], since $V_f'(t_r)$ is a function of the slope of the signal rather than its level. In Fig. 10, the digitized step $V_f(t_r)$ and the transformed signal $V_f'(t_r)$ are shown for representative data. The difference between $V_f(t)$ (Fig. 5) and $V_f(t_r)$ (Fig. 10a) is due to the antialiasing filter (this was confirmed by sampling at a higher frequency and increasing the filter bandpass). The accelerometer signals are passed through identical processing. Because of cancellation of the antialiasing filter and digital filter (Z_s) characteristics, an output/input, $\bar{V}_a'(\omega_r)/\bar{V}_f'(\omega_r)$, approximates $\bar{a}_j(\omega)/\bar{f}_k(\omega)$.

In both of the above techniques, exponential windows could be used to reduce leakage if the filtered response signals do not decay sufficiently in the observation window of the Fourier transform.

Frequency-response functions were obtained using both methods for the space mast data. They were essentially identical over the frequency range explored (1-20 Hz). We do not see any fundamental reason why one technique would be better than the other with regard to precision. However, the analog filtering can be done more rapidly than the digital transformations of Eq. (18) when using Modal-Plus software, and, consequently, the overall processing time is significantly longer when digital filtering is used.

The test of the space mast (Fig. 4) thus yields a matrix of frequency-response functions, $\bar{H}_{jk}(\omega_r)$, with $j=1,\ldots,18$ and $k=1,\ldots,3$. Verification of linearity by checking for reciprocity [i.e., checking that $\bar{H}_{ij}(\omega_r)$ and $\bar{H}_{ji}(\omega_r)$ are equal] is possible and is one of the advantages of this implementation of step relaxation. Examples of this type of check are given in Ref. 4.

Parameter Identification Using a Complex Exponentials Method

The next step is to determine the structure's modal parameters from the measurement-based $\bar{H}_{jk}(\omega_r)$. This was accomplished with the polyreference algorithm of the Structural Dynamics Research Corporation software for the space mast data.

In the polyreference technique, the measurement-based frequency-response functions, $\bar{H}_{jk}(\omega_r)$, obtained as described in the previous section, are first inverted to the time domain over the frequency range of interest with an FFT algorithm, thus obtaining measurement-based unit impulse response functions, denoted herein as $H_{jk}(t_r)$. Then, parameters λ_p (the complex poles) and A_{jk}^p (the residues) are found that result in a best least-squares fit of the analytic expression

$$H_{jk}(t) = \sum_{p=1}^{2n} A_{jk}^p e^{\lambda_p t} \tag{19}$$

to the measurement-based $H_{jk}(t_r)$. The modal frequencies and damping factors are calculated from the λ_p. The mode

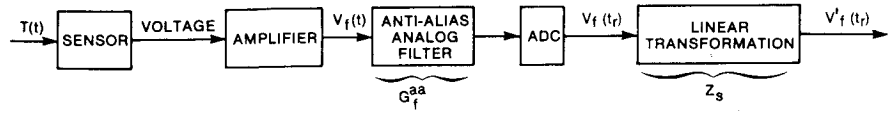

Fig. 9 Preprocessing of $T(t)$ with linear transformations, Z_s.

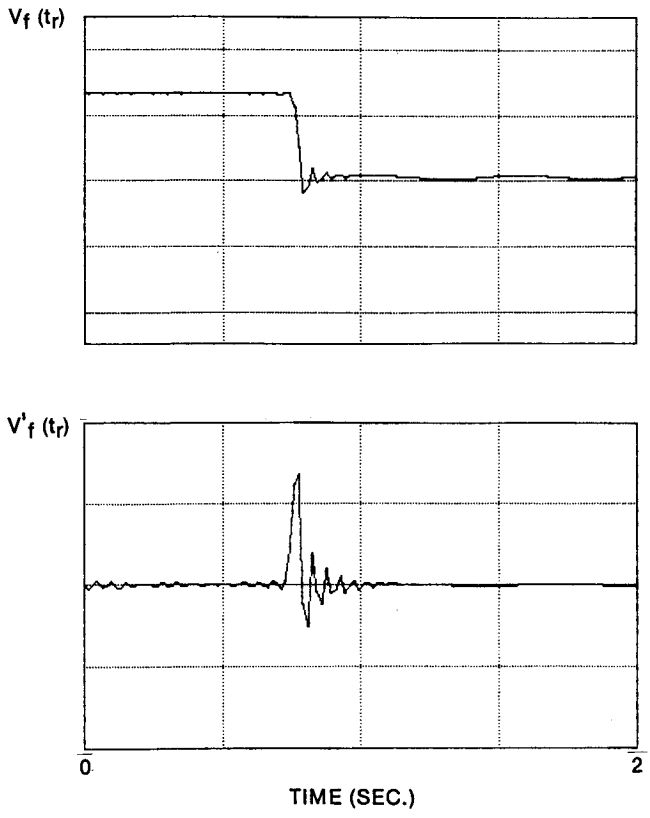

Fig. 10 $V_f(t_r)$ and $V_f'(t_r)$.

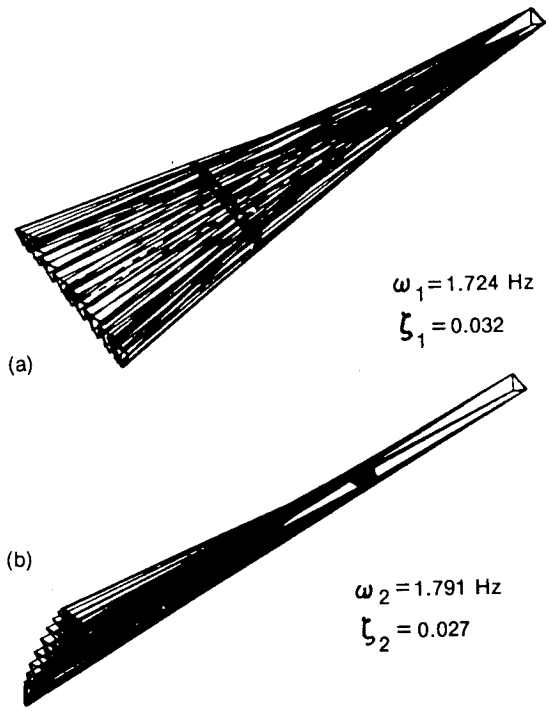

Fig. 11 Successive frames of the animation of the two fundamental bending modes derived in case a.

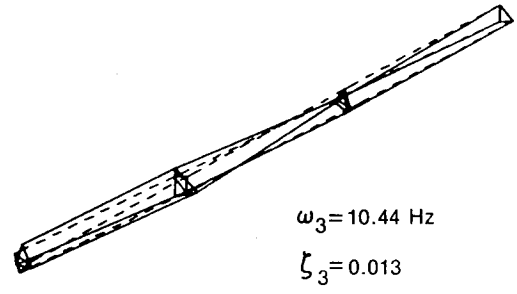

Fig. 12 First torsion mode derived in case b.

shapes and relative scale factors (modal masses) are calculated from the residues, A_{jk}^p. The algorithms in the polyreference software that provide estimates of the poles and residues are based on the Prony-type implementation of the complex exponentials method. The practical implementation and characteristics of this type of algorithm in both time- and frequency-domain formulations are demonstrated in Refs. 10-13, mainly for single-input data [scalar element or column of $H(t_r)$]. The Prony method is demonstrated to have good performance for multimode estimation in practical situations. It is sensitive to noise in the data; least-squares data smoothing results in significant bias errors in damping estimates. The technique has been shown to be closely related to the Auto-Regressive Moving Average (ARMA) and other methods.[12,14,15] The polyreference technique[16] is an implementation of the Prony algorithm in the time domain that includes the multi-input case (i.e., the curve fit can be done for scalar element, column or multiple-column data, as appropriate).

Successful application of the polyreference method requires a certain amount of user-interactive computer processing and trial and error, with the frequency range of $H(\omega)$ and the order n [Eq. (19)] as variables. The iterative procedures are illustrated to some extent in Ref. 17. A description of the detailed procedures is beyond the scope of this paper. However, to illustrate the capacity of the method in the context of step relaxation, the main processing features and results are given for the aforementioned space mast data.

The mast has two cantilever-like transverse bending modes (X and Y directions) at about 2 Hz and three modes (two transverse bending and one torsion) at about 10 Hz. To successfully process these two clusters of closely spaced modes with the polyreference software, the following combinations of data and bandwidth were needed. a) To obtain the lowest two bending modes, two columns of $H(\omega)$ generated with nonparallel force inputs (in the X-Y plane) were needed, together with a limitation on the frequency range of 1-5 Hz. b) To obtain the three modes near 10 Hz, three columns of $H(\omega)$ generated with three force inputs designed to induce significant transverse bending and twist were needed. It was further necessary to limit the processing frequency range to 8.5-16 Hz. Further details of these two cases are given in Table 1.

The modal parameters obtained in case (a) above are shown in Fig. 11. The two modal frequencies are very closely spaced, and the damping factors are substantially different. The modes have the appearance of being orthogonal to each

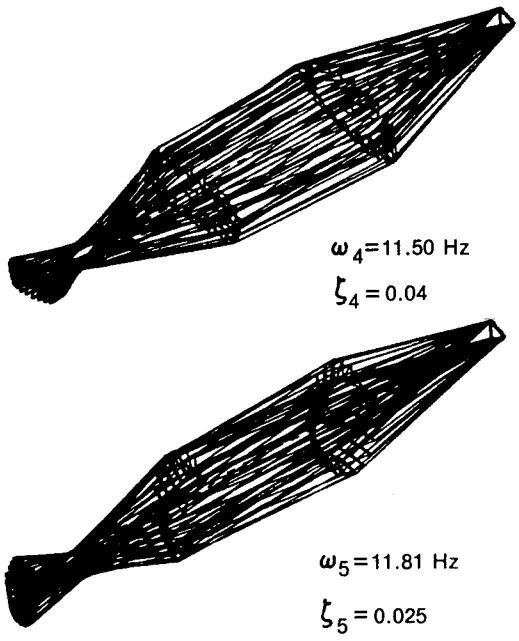

Fig. 13 Successive frames of an animation of the second bending modes derived in case b.

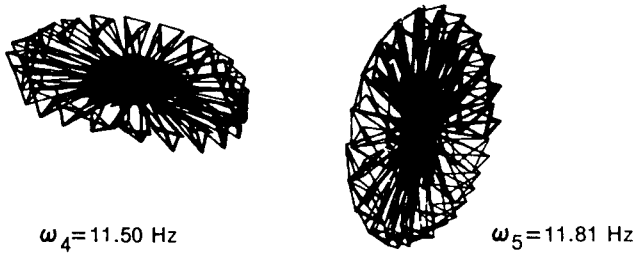

Fig. 14 End view of the modes of Fig. 13. Bending and rotation of the tip are observable.

other. The modal assurance criterion[18] (which is essentially the square of the correlation coefficient between the two shapes) is calculated to be 0.014, thus confirming that the shapes were not correlated.

In processing the data of case (b) above, 22 poles were initially derived using the polyreference routine. Of these, all except six could easily be disregarded as noise-induced computational poles. By use of mode shape plots, animation, and the modal assurance criterion, the six modes were further classified into three independent and three physically sensible but dependent modes. The three independent modes were essentially fundamental torsion at 10.44 Hz, and second bending $-X$ at 11.50 Hz and $-Y$ at 11.81 Hz. The modes are depicted in Figs. 12-14. A graph of the corresponding curve fit is shown in Fig. 15. The modal assurance criterion of the three modes is given in Table 2, and it confirms the independence of the shapes.

Several combinations of $\bar{H}(\omega)$ columns and bandwidth, other than those of Table 1, were processed with polyreference with less than satisfactory results. For example, the following were not successful: 1) attempts to process data from two or three inputs with the total available bandwidth (1-16 Hz), 2) attempts to extract the two fundamental bending modes with one data column, 3) attempts to extract the three modes near 10 Hz with only two columns of H. The latter two attempts conform with a principle that, to extract repeated roots, one requires as many columns of the H matrix as the multiplicity of the root.

The results presented herein demonstrate the limit of what is achievable by step relaxation with a single force input for this particular structure. Although excellent performance was obtainable in the range of 0-20 Hz, the method was not successful for modes above 20 Hz (modes between 10 and 60 Hz were obtainable with other methods), since not enough energy was input into the structure for these higher frequencies.

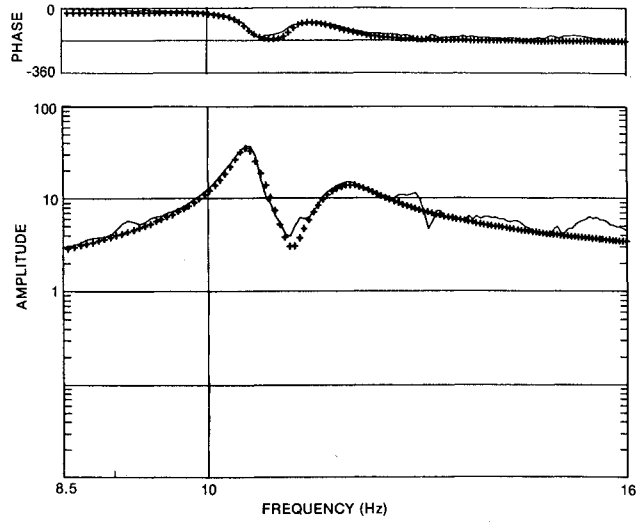

Fig. 15 Curve fit of experimental data (continuous curve) at driving point 8Y for case b.

Table 1 Description of conditions leading to acceptable parameter estimation

Case	Modes sought	Location/direction of force inputs, Y	Frequency range of processing, Hz
a	First bending-X	$8Y$	1.0-4.7
	First bending-Y	$-9Y$	
b	First torsion	$11Y$	8.5-16
	Second bending-X	$8Y$	
	Second bending-Y	$-9Y$	

Table 2 Modal assurance criterion between first torsion mode and second bending modes

	3	4	5
3	1.000	0.001	0.010
4		1.000	0.001
5			1.000

Concluding Remarks

The theory and practical aspects of an implementation of the step relaxation method that includes preprocessing of data in the frequency domain have been outlined. The method appears to be well suited for modal test of large flexible structures where the lower frequency modes are of prime interest.

As noted in the introduction, step relaxation may also be implemented directly with time-domain data by processing free decay time histories with a complex exponentials method as in Ref. 3, for example. With the direct method, potential errors associated with the fast Fourier transform are avoided, and thus weakly excited modes might be better detected. The frequency-domain-based method, on the other hand, offers the advantages over the direct time-domain method of permitting frequency-domain averaging of several trials to reduce noise, and of enabling the modal masses to be determined. Also, the frequency-domain-based method is more compatible with the wide choice of recently developed commercial fast-Fourier-transform-based modal analysis equipment and software.

In addition to the test of the space mast given herein as an example, the step relaxation method has been used at the authors' organization for modal survey of an ultrahigh-frequency satellite antenna, a deployable solar array, and the lower modes of a seismic block.

References

[1]Ramsey, K. A., "Effective Measurements for Structural Dynamics Testing," *Sound and Vibration*, Pt. II, April 1976, pp. 18-31.

[2]Lauffer, J. P., Carne, T. G., and Nord, A. R., "Mini-Modal Testing of Wind Turbines Using Novel Excitation," *Proceedings of the Third International Modal Analysis Conference*, Orlando, FL, Vol. 1, 1985, pp. 451-458.

[3]Carne, T. G., Martinez, D. R., and Ibrahim, S. R., "Modal Identification of a Rotating Blade System," *Proceedings of the 24th Structures, Structural Dynamics and Materials Conference*, Lake Tahoe, NV, Pt. 2, 1983, pp. 728-736.

[4]Mutch, G. F., Vigneron, F. R., and Vold, H., "The Dynamic Analysis of a Space Structure via the Use of Step Relaxation Testing," *Proceedings of the 2nd International Modal Analysis Conference*, Orlando, FL, 1984, pp. 368-377.

[5]*Modal-Plus Users Manual*, Vers. 8.0, Structural Dynamics Research Corporation, Cincinnati, OH, 1983.

[6]Papoulis, A., *The Fourier Integral and Its Applications*, McGraw-Hill Book Co., New York, 1962, Chaps. 3, 5, 6.

[7]Bracewell, R., *The Fourier Transform and Its Applications*, McGraw-Hill Book Co., New York, 1965.

[8]Soucy, Y. and Vigneron, F. R., "Identification of Structural Properties of a Continuous Longeron Space Mast," *Proceedings of the AIAA/ASME/ASCE/AHS 25th Structures, Structural Dynamics and Materials Conference*, Palm Springs, CA, Pt. 2, May 1984, pp. 130-139.

[9]Oran Brigham, E., *The Fast Fourier Transform*, Prentice-Hall, Englewood Cliffs, NJ, 1974, Chaps. 5 and 6.

[10]Van Blaricum, M. L. and Mittra, R., "Problems and Solutions Associated with Prony's Method for Processing Transient Data," *IEEE Transactions on Antennas and Propagation*, Vol. AP-26, Jan. 1978, pp. 174-182.

[11]Poggio, A., Van Blaricum, M. L., Miller, E. K., and Mittra, R., "Evaluation of a Processing Technique for Transient Data," *IEEE Transactions on Antennas and Propagation*, Vol. AP-26, Jan. 1978, pp. 165-173.

[12]Dudley, D. G., "Parametric Modeling of Transient Electromagnetic Systems," *Radio Science*, Vol. 14, May-June 1979, pp. 387-396.

[13]Brittingham, J. N., Miller, E. K., and Willows, J. L., "Pole Extraction from Real-Frequency Information," *Proceedings of IEEE*, Vol. 68, Feb. 1980, pp. 263-273.

[14]Sakar, T. K., Weiner, D. D., Nebat, J., and Jain, V. K., "A Discussion of Various Approaches to the Identification/Approximation Problem," *IEEE Transactions on Antennas and Propagation*, Vol. AP-30, Jan. 1982, pp. 89-98.

[15]Leuridan, J. and Vold, H., "A Time Domain Linear Model Estimation Technique for Multiple Input Modal Analysis," American Society of Mechanical Engineers, Winter Annual Meeting, Nov. 1983, AMD-Vol. 59, pp. 51-62.

[16]Vold, H., Kundrat, J., Rocklin, G. T., and Russel, R., "A Multi-Input Estimation Algorithm for Minicomputers," SAE Tech. Paper 820194, 1982.

[17]Crowley, S. M. and Allemang, R. J., "Applications of the Poly-reference Technique in Experimental Modal Analysis," *Proceedings of the 2nd International Modal Analysis Conference*, Orlando, FL, Feb. 1984, pp. 111-117.

[18]Allemang, R. J. and Brown, D. L., "A Correlation Coefficient for Modal Vector Analysis," *Proceedings of the 1st International Modal Analysis Conference*, Orlando, FL, Nov. 1982, pp. 110-116.